

The Problem

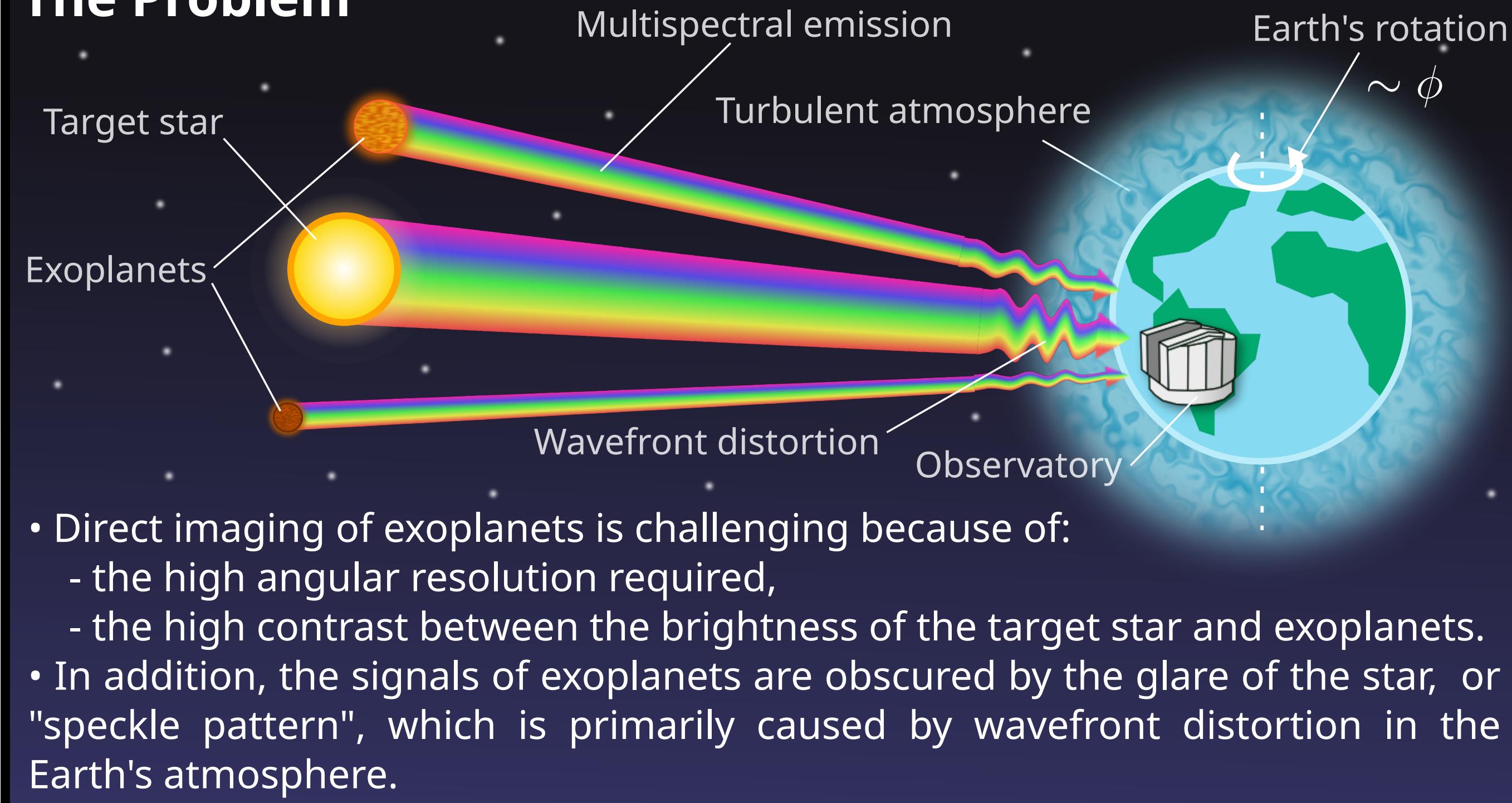
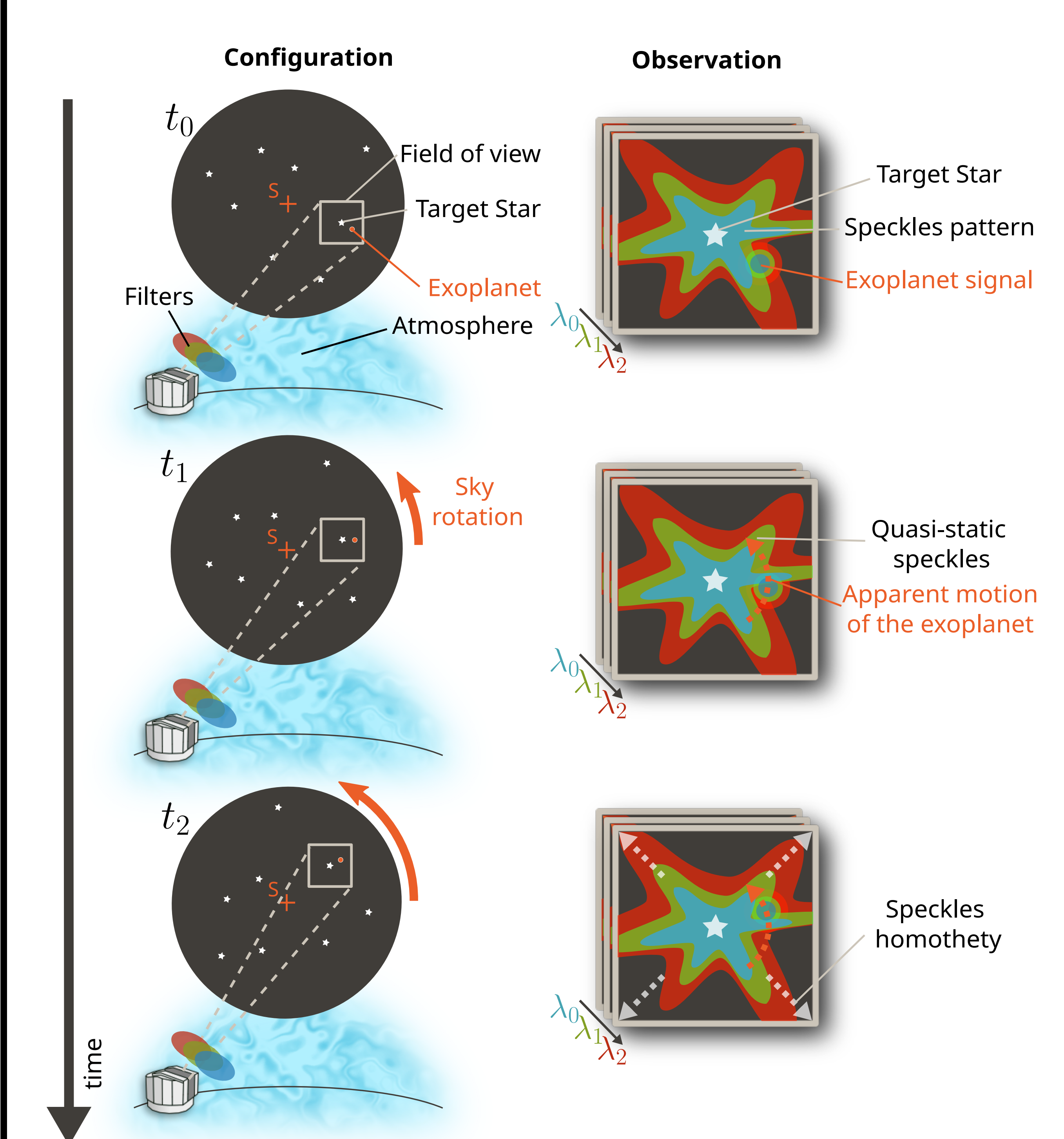
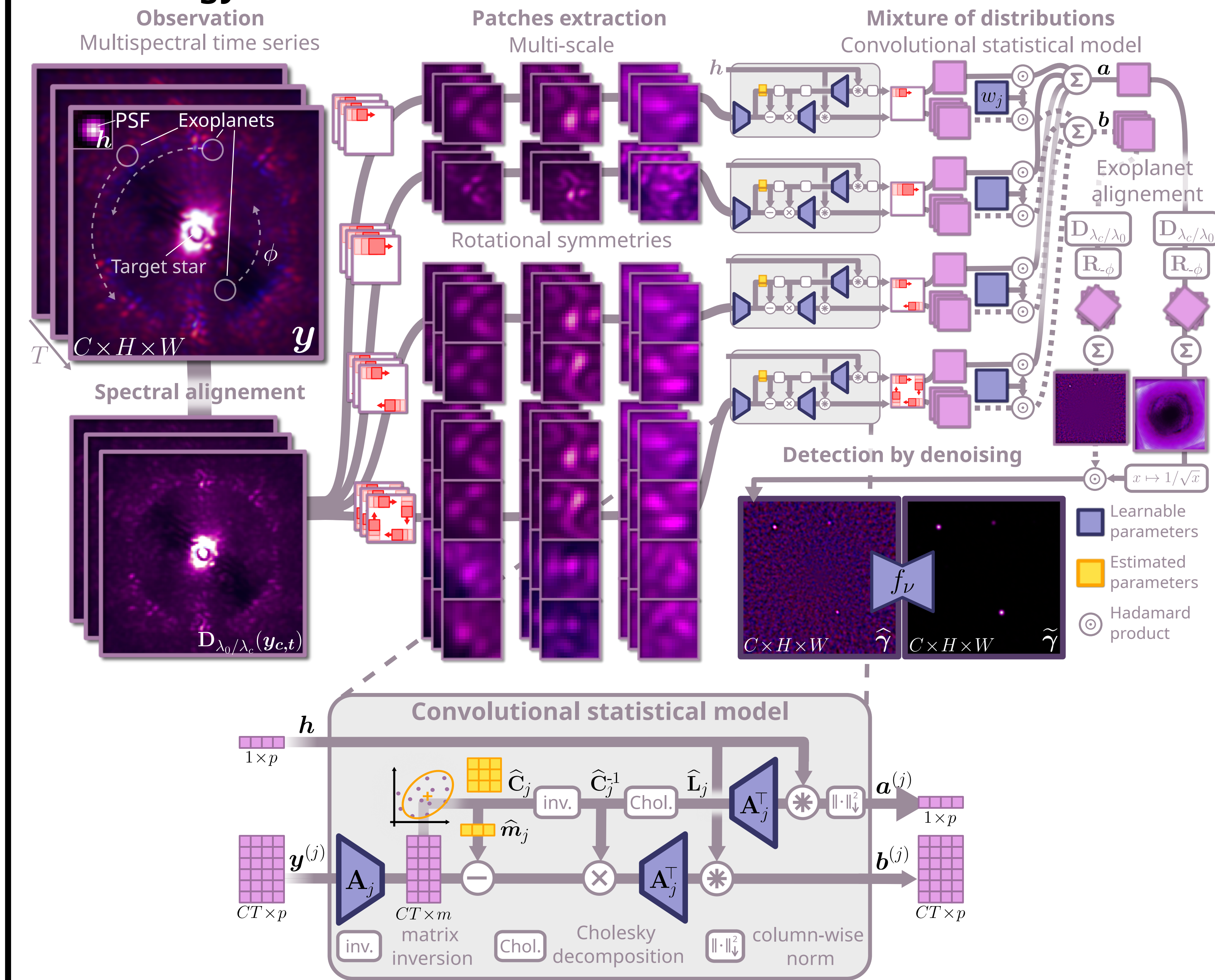


Image Formation Model



- The natural rotation of the Earth causes an apparent motion of the exoplanet signal, while speckles remain quasi-static.
- Because of diffraction, the relationship between speckle patterns at different wavelengths can be approximated by a homothety.

Methodology



The proposed architecture recovers the flux of exoplanets by solving:

$$\hat{\alpha} = \arg \min_{\alpha \in \mathbb{R}^{H \times W}} \underbrace{\varphi_{\theta}(\alpha, \chi(y))}_{\mathbf{A}} + \underbrace{\psi_{\nu}(\alpha)}_{\mathbf{B}}$$

A. Learnable prior on the speckles: our convolutional statistical model combines distributions at multiple scales, joint spectral modeling, and physics-based symmetries. The objective function writes:

$$\varphi_{\theta}(\alpha, x_0, \chi(y)) = \prod_t \prod_{j \in S(x_t)} \mathbb{P}(A_j(y_t^{(j)} - \alpha h^{(j)}(x_t)) | \hat{m}_j, \hat{C}_j)^{w_j}$$

and admits a closed-form optimum:

$$\hat{\alpha} = \frac{\sum_t b_t(x_t)}{\sum_t a_t(x_t)}$$

$$\hat{\sigma}_{\alpha} = \frac{1}{\sqrt{\sum_t a_t(x_t)}}$$

where:

$$a(x_t) = \sum_{j \in S(x_t)} w_j h^{(j)}(x_t)^T A_j^T \hat{C}_j^{-1} A_j h^{(j)}(x_t)$$

$$b_t(x_t) = \sum_{j \in S(x_t)} w_j h^{(j)}(x_t)^T A_j^T \hat{C}_j^{-1} (A_j y_t^{(j)} - \hat{m}_j)$$

B. Learnable prior on the exoplanet signal: implemented by denoising the detection map ($\hat{\gamma} = \hat{\alpha} / \hat{\sigma}_{\alpha}$) resulting from **A**.

The architecture is trained end-to-end, by injecting synthetic exoplanets into real observations, and maximizing the log-likelihood of the predicted flux.

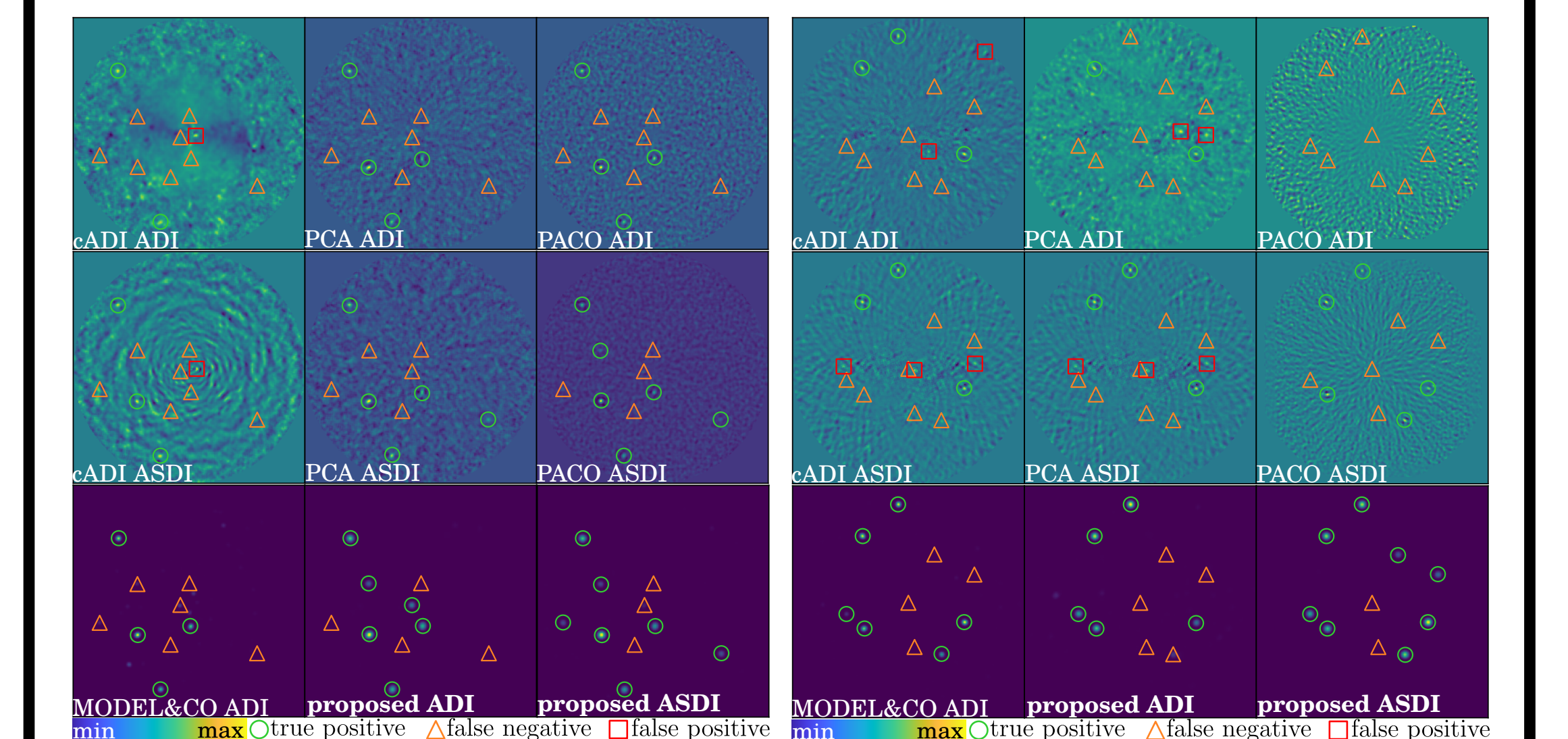
Results

Detection performance

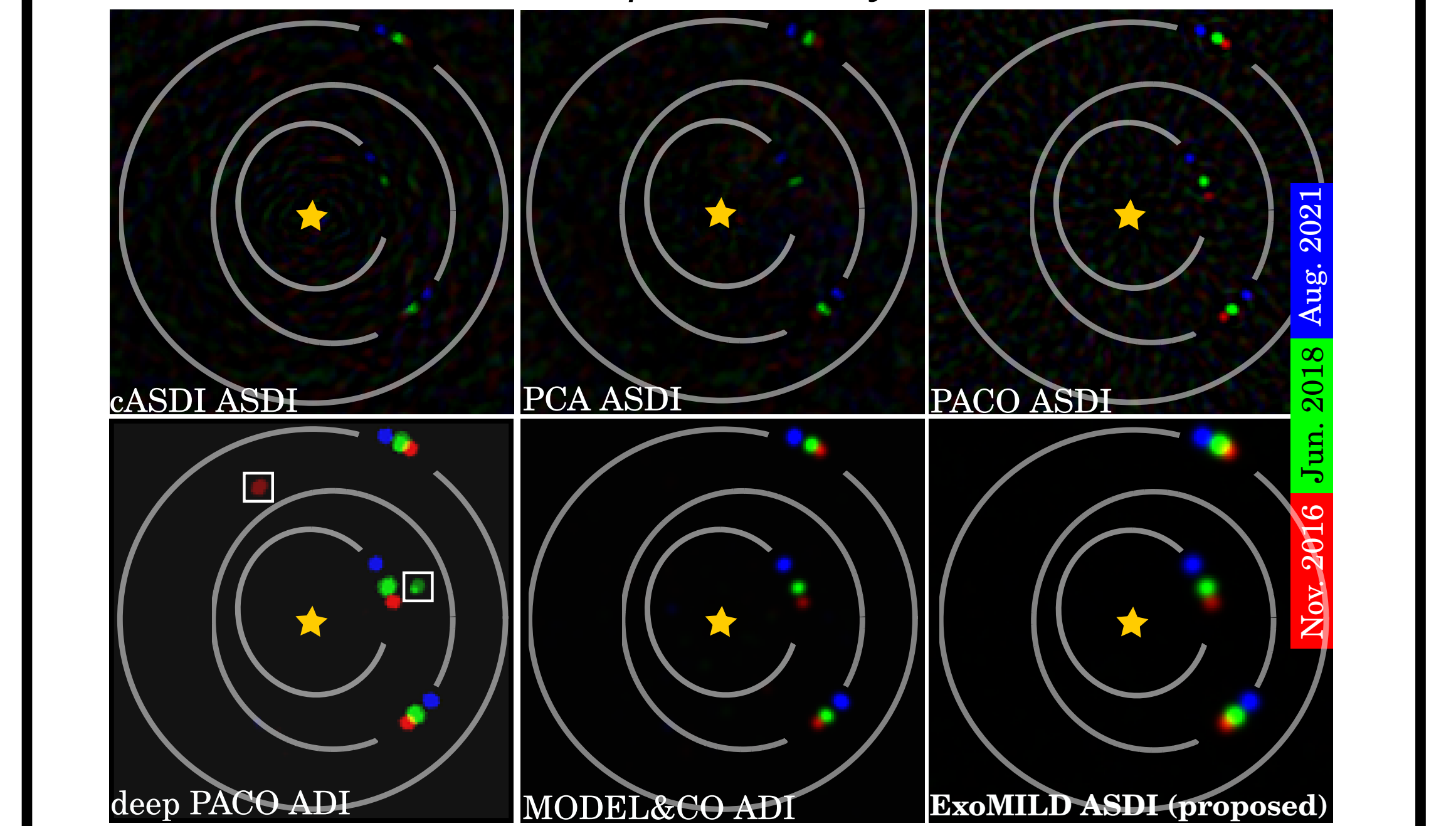
Method	HD159911 (54°)	HD216803 (23°)	HD206860 (11°)	HD188228 (6°)	HD102647 (2°)	average AUC
cASDI	0.288 ± 0.014	0.422 ± 0.007	0.489 ± 0.010	0.303 ± 0.014	0.343 ± 0.009	0.369 ± 0.005
PCA	0.634 ± 0.010	0.643 ± 0.011	0.505 ± 0.009	0.392 ± 0.011	0.218 ± 0.011	0.478 ± 0.005
PACO	0.629 ± 0.006	0.669 ± 0.012	0.579 ± 0.015	0.517 ± 0.015	0.207 ± 0.012	0.520 ± 0.006
MODEL&CO	0.653 ± 0.010	0.731 ± 0.011	0.646 ± 0.012	0.638 ± 0.014	0.554 ± 0.009	0.645 ± 0.005
Proposed	0.673 ± 0.009	0.740 ± 0.010	0.661 ± 0.012	0.631 ± 0.013	0.518 ± 0.012	0.645 ± 0.005

Method	HD159911 (54°)	HD216803 (23°)	HD206860 (11°)	HD188228 (6°)	HD102647 (2°)	average AUC
cASDI	0.448 ± 0.009	0.537 ± 0.013	0.451 ± 0.007	0.352 ± 0.017	0.294 ± 0.012	0.417 ± 0.006
PCA	0.694 ± 0.013	0.696 ± 0.007	0.552 ± 0.011	0.398 ± 0.011	0.236 ± 0.009	0.515 ± 0.005
PACO	0.698 ± 0.015	0.768 ± 0.008	0.710 ± 0.014	0.700 ± 0.009	0.589 ± 0.014	0.693 ± 0.005
Proposed	0.731 ± 0.009	0.804 ± 0.013	0.747 ± 0.010	0.782 ± 0.008	0.744 ± 0.006	0.761 ± 0.004

AUC-ROC evaluated on semi-synthetic data



Detection maps on semi-synthetic data



Detection maps obtained on real exoplanets (HR 8799 system)

Characterization performance

Method	flux error (ARE)	position error (RMSE)
PACO	0.56	0.21
Proposed	0.51	0.11

- [1] Bodrito+ "MODEL&CO: Exoplanet detection in angular differential imaging by learning across multiple observations" MNRAS 2024.
- [2] Flasseur+ "Exoplanet detection in angular differential imaging by statistical learning of the nonstationary patch covariances" A&A 2018.
- [3] Marois+ "Angular differential imaging: a powerful high-contrast imaging technique" A&A 2006.